Measurements of relative intensity noise (RIN) in semiconductor lasers

Irène Joindot

Classification
Physics Abstracts
42.60

Measurements of relative intensity noise (RIN) in semiconductor lasers

Irène Joindot

CNET-LAB/OCM, route de Trégastel, BP 40, F-22301 Lannion, France

(*Received 14 November 1991, accepted 30 March 1992*)

Abstract. — The intensity fluctuations of the laser diodes light are characterized by the so-called *relative intensity noise* (RIN). In this paper a very accurate measurement technique is presented and results are given on some components. RIN measurements on isolated longitudinal modes can explain how the energy is shared between the modes.

Introduction.

Like other electronic devices, semiconductor lasers exhibit noises. A semiconductor laser is an imperfect optical oscillator, emitting waves, the results of which are described by an electric field affected by amplitude or intensity noise (the topic of this paper), and phase or frequency noise. The origin of these noises must be sought in the discontinuous nature of the photons absorption and emission, and the carrier generation and recombination processes.

The intensity fluctuations of the light beam emitted by a laser diode, even when it is CW biased in a very stable manner, impress an ultimate limit to any optical communication system. Briefly speaking, intensity fluctuations are more important in direct detection systems, while phase fluctuations are more important in coherent systems especially when a balanced heterodyne receiver is used to cancel the local oscillator intensity noise.

The parameter which describes the intensity noise is called RIN (Relative Intensity Noise). It ought to appear now in data sheets. The reason for this new interest has been brought about the recent idea of using semiconductor lasers in lightwave multi-channel analog amplitude modulation video distribution systems, in the 10 MHz-800 MHz band. The necessary signal-to-noise ratio requires a RIN value as low as – 155 dB/Hz [1]. In this paper, the described measurement technique can reach RIN values as low as – 170 dB/Hz.

Finally, the aim of noise investigations as a function of frequency is to know the intrinsic bandwidth without the parasitic elements circuit.

1. Theoretical re-calls on intensity fluctuations of optical sources.

The noise spectral density of the photocurrent fluctuations at the output of a detector illuminated by an optical source is the sum of two terms [2] :

$$w_{\Delta i}(f) = 2 \cdot q \cdot I_{\text{ph}} + I_{\text{ph}}^2 \cdot \text{RIN}\ (f) \qquad (1)$$

where *RIN* means « Relative Intensity Noise » :

$$\text{RIN}\ (f) = \frac{W_{\Delta\mathfrak{I}}(f)}{\langle \mathfrak{I} \rangle^2} \tag{2}$$

I_{ph} is the average value of the output photocurrent, q is the electron charge, $\langle \mathfrak{I} \rangle$ is the average intensity of the optical field, $W_{\Delta\mathfrak{I}}(f)$ is the power spectral density of the optical intensity fluctuations.

The first term of relation (1), well known as « shot noise », is the result of the discontinuous nature of electrons and photons. In the second term the one-sided power spectral density of the relative fluctuations of the optical source called RIN, appears : it is a parameter of the optical source and not of the detector. And so, to know more about RIN, it is necessary to examine the optical source.

When a detector is illuminated by a perfect amplitude stabilized laser, the power spectral density of the fluctuations of the light intensity is equal to zero and the noise of the photocurrent is a pure shot noise. Let us examine some other optical sources.

The light emitted by incoherent thermal sources consists of the superposition of elementary independent fields which arise when different atoms spontaneously emit light [3]. The RIN is equal to the coherence time τ_C of the source. Light emitting diodes (LED) are thermal Gaussian sources. The optical bandwidth $\Delta\lambda$ of a surface emitting LED lies between 400 and 600 Å around 1 μm emitted wavelength : $1/(\pi\tau_C) \approx 30 \,.\, \Delta\lambda$ (Å).

So a surface emitting LED will be used to calibrate our RIN measurement set-up, that is to say, to measure pure shot noise, because with such a source, the second term of the right member of equation (1) is much lower than the first term : shot noise is much higher than excess noise due to the optical source. But according to the optical bandwidth, the photocurrent must not exceed 100 or 200 μA.

A superluminescent diode (SLD) is an incoherent source with an internal gain [4]. Its optical output power is much higher than the LED optical power and its optical spectral bandwidth much lower than the LED bandwidth. Thusfar, when a detector is illuminated by a SLD, excess noise can be observed above the pure shot noise, as it will be shown later. So we cannot measure pure shot noise with a SLD.

In the early seventies, semiconductor laser diodes were considered as crude devices, but now, buried structures (BH) and distributed feedback structures (DFB) can compete with solid state or gas lasers. The next paragraphs will be devoted to noise properties of semiconductor laser diodes.

2. Modelisation of intensity noise in semiconductor lasers.

The spectral density of the quantum fluctuations of the photons and electrons population is usually obtained by adding to the well-known rate equations, Langevin fluctuations operators having shot noise character [9] : $f_N(t)$ for electrons and $f_S(t)$ for photons. In hypothesis, the noise sources $f_N(t)$ et $f_S(t)$ are Gaussian random processes and their auto- and crossrelation functions are proportional to Dirac distributions. Each process such as absorption or emission of a photon, or arrival or departure of an electron from the conduction band is a source of shot noise. They are uncorrelated noise sources and their variances add. Rate equations are linearized, assuming a small increment around stationary value and s_i being the total number of photons in the i-th mode at wavelength λ_i, we will write :

$$s_i(t) = S_i + \Delta s_i(t) \,. \tag{3}$$

At first we will consider a single mode laser. In the frequency domain, it is easy to calculate

the two-sided power spectral density of the fluctuations of photons number $\langle[\Delta s(\Omega)]^2\rangle$, where $\Omega = 2\pi f$, f being the baseband frequency at which the noise is analysed (for further details, see [2]). The expression of $\langle[\Delta s(\Omega)]^2\rangle$ contains a denominator which can be written as $(f^2 - f_R^2)^2 + (\Theta/2\pi)^2 . f^2$ and reveals a resonance frequency f_R and a damping factor Θ. f_R and Θ have the same expression as the resonance frequency and damping factor of the modulation response modelisation.

The inversion population parameter helps to express resonance frequency and damping factor in a simple manner. This parameter is defined as follows :

$$n_{pop} = \frac{N_S}{N_S - N_0} \tag{4}$$

where N_s is the electron number at threshold and N_0 the electron number at transparency. This parameter equals to 1 in a totally inverted laser and lies between 2 or 3 in a semiconductor laser.

So above threshold (more than 20 %), a simplified expression of the resonance frequency can be derived :

$$f_R^2 = \frac{1}{4 . \pi^2} \cdot \frac{n_{pop}}{\tau_\phi . \tau_S} \cdot \left(\frac{I}{I_S} - 1 \right) \tag{5}$$

where I is the injection current, I_s the threshold current, τ_ϕ is the photon lifetime, and τ_s is the spontaneous radiative recombination lifetime. f_R^2 is proportional to $I/I_s - 1$.

The damping factor is dominated by extra effects like carriers diffusion [5] or gain compression by the photons of the powerful mode [6] : gain compression increases the damping factor.

Deriving the exact expression of RIN is rather tedious and cumbersome but a crude and very simple approximation can be found [2] at zero frequency and between 20 and 30 % above threshold (with an error less than 10 %), where β is the fraction of spontaneous emission injected into the mode :

$$\text{RIN} = 2 \cdot \frac{\langle[\Delta s]^2\rangle}{S^2} \tag{6}$$

$$= \frac{4 . \beta . \tau_\phi}{n_{pop}^2 . (I/I_S - 1)^3} \tag{7}$$

RIN decreases like $(I/I_S - 1)^{-3}$ or like the output power to the minus 3 (the output power being proportional to $I/I_S - 1$).

3. Experimental techniques.

3.1 NOISE MEASUREMENT EXPERIMENTAL SET UP. — Measurements of relative intensity noise have been carried out, in our laboratory for many chips on submount lasers, emitting in a single transverse mode, using the well-known single-detector technique. The experimental set-up is shown in figure 1. To lower the optical feedback, the light output power is first reduced by an optical attenuator, slightly tilted off axis, and is collected through a long working distance microscope objective (MO). The photodiode (PIN) photocurrent is sequentially fed into a lock-in amplifier either through a 1 kΩ resistance, either through a low frequency (30 MHz with 1 MHz bandwidth) noise measurement channel, or through a high frequency (800 MHz to 10 GHz) noise measurement channel with a local oscillator. The low

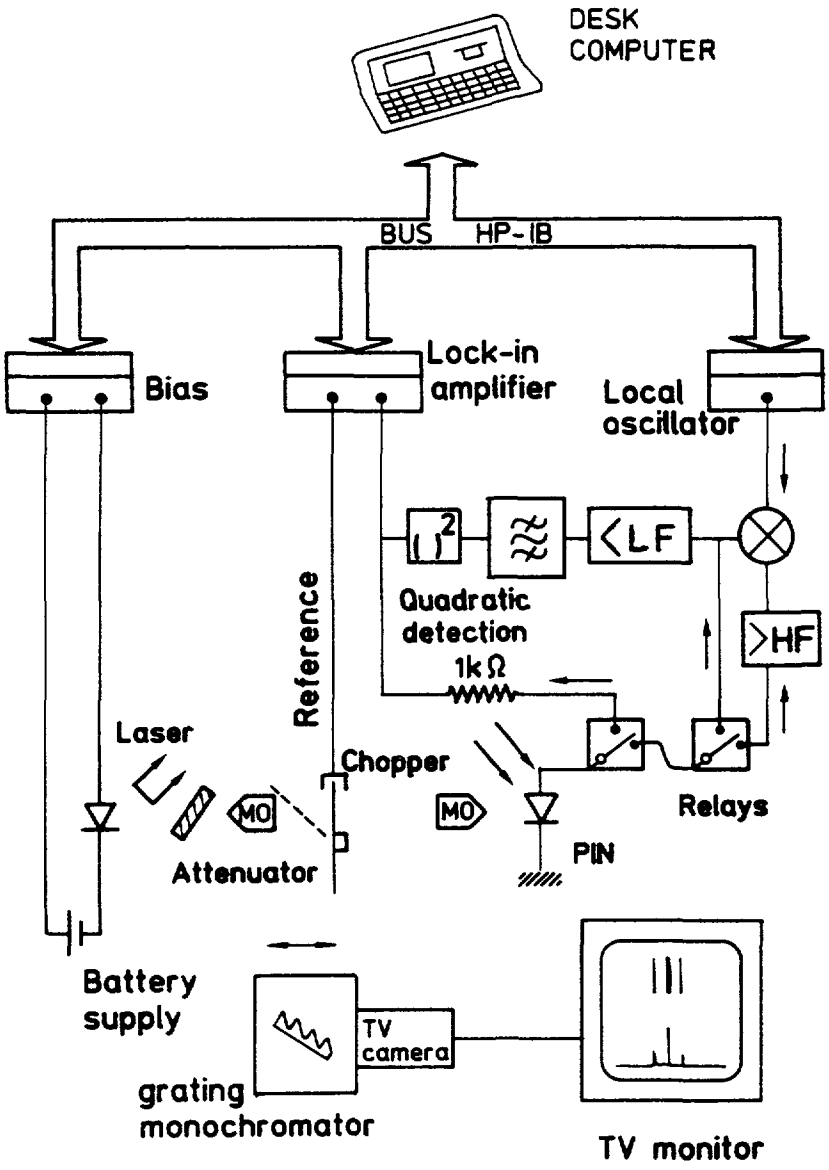

Fig. 1. — Experimental set-up.

frequency measurement channel consists of a Trontech L30B amplifier followed by a 3 dB attenuator, a 30 MHz Telonic filter, a SCD Nuclétude amplifier and a 10 dB attenuator. A Nuclétude wideband amplifier is the first stage of the high frequency measurement channel. Then the local oscillator is launched through a RF mixer. This channel is ended by a 30 MHz Telonic filter and a 6 dB attenuator. Finally, the 30 MHz channel is used as the intermediate frequency amplifier.

A desk computer drives the sequences, selects the lock-in best scale, gathers and averages the photocurrent, the corresponding noise level values and the zero (darkness) noise of the electronics, after stepping up the laser current.

Eventually, a Jobin-Yvon optical spectrometer (HRS1000) is used to select one or two longitudinal modes to perform partition noise or cross-relation measurements, as will be shown at the end of this paper.

3.2 RIN (RELATIVE INTENSITY NOISE) MEASUREMENTS. — At first we calibrate our experimental set-up using an incoherent source : a surface light emitting diode at 0.85 or 1.3 μm. We check that, at each frequency, pure shot noise with a power spectral density proportional to the photocurrent I_{ph} is obtained. Then the LED is replaced by the laser and excess noise appears above the shot noise, especially at laser threshold. With this calibration process, RIN measurements results are only dependent on the exact value of the photocurrent, as shown by the following expression :

$$\mathrm{RIN} = \frac{2 \cdot q}{I_{ph}} \left(\frac{\langle \Delta i^2 \rangle}{\langle \Delta i_{sh}^2 \rangle} - 1 \right) \tag{8}$$

$\langle \Delta i^2 \rangle$ is the noise spectral density when the detector is illuminated by the laser and $\langle \Delta i_{sh}^2 \rangle$ when it is illuminated by the LED. The ratio between the two noise terms cancels the conversion factor between noise level and voltage level at the output of the synchronous amplifier. Noise data and photocurrent data are accumulated as long as the required accuracy is not obtained. With this experimental technique we can measure RIN values as low as − 170 dB/Hz with a 20 % error if the photocurrent is higher than 200 μA and if there are 200 accumulated data.

In figure 2, we can see the noise spectral density when the detector is illuminated by a LED, a SLD and a laser (LD) : the noise obtained with a SLD is different from pure shot noise.

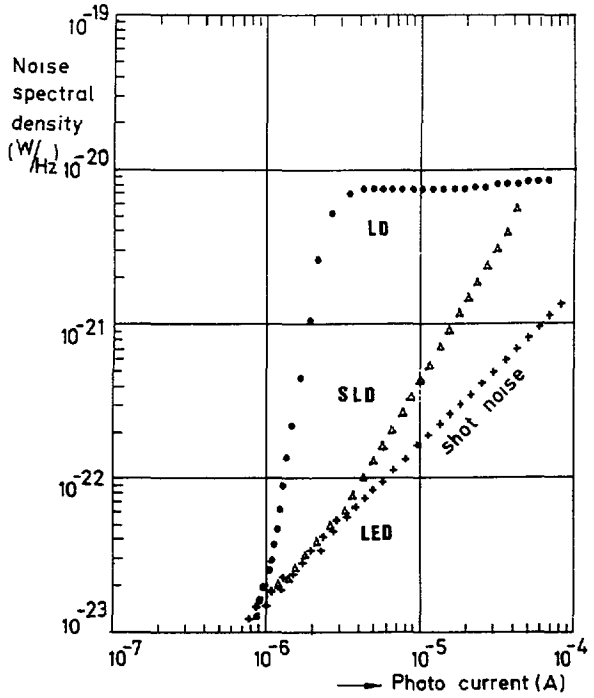

Fig. 2. — Noise spectral density, at 30 MHz, when the detector is illuminated by a laser diode (LD), a superluminescent diode (SLD) and a light emitting diode (LED), *versus* photocurrent.

4. Global noise measurements.

Global noise means that all the modes are gathered on the detector, while when the modes are separated by a dispersive medium (for instance a spectrometer), the noise induced by the share of intensity is called « mode partition noise ».

4.1 General features of the noise.

4.1.1 *Noise as function of frequency.* — At low frequency, from 0 to around 50 kHz, the noise has a $1/f$ behaviour as in any semiconductor device. Then, up to some hundreds of megaHertz, the noise exhibits a flat, and beyond 1 GHz a peak with a maximum corresponding the relaxation frequency between photons and electrons in the cavity, and at the end the decreasing steepens. The peak frequency increases with the injection current above the threshold.

4.1.2 *Noise as function of injection current.* — In the flat region of the spectrum (50 kHz-300 MHz), the relative intensity noise reaches its smallest value. As a function of the injection current, the RIN increases as the output power P under the threshold, then decreases like P^{-3} just above the threshold (in agreement to relation (7)) and like P^{-1} far from the threshold. It is possible to explain this behaviour as follows : under the threshold, the laser can be considered as an incoherent thermal light source with a narrow optical bandwidth and at that moment its RIN increases with its coherence time, this coherence time being inversely proportional to the optical bandwidth. The small gain just before the threshold reduces the optical spectrum and so increases the noise without bringing any stability. Then above the threshold, the gain saturation leads a stabilization of electrons fluctuations and then of photons relative fluctuations. The light stimulation effect is to synchronize the emission of the electrons. Consequently, the noise peak at threshold shows the turning of light properties when stimulated emission overcomes spontaneous emission.

4.2 At middle frequency.

— Noise measurements at middle frequency, that is to say in the flat region (30 MHz), reveal the laser stability : the weaker the RIN is, the higher the stability is. In the two following sections we will set gain guiding lasers over against index guiding lasers, then multimode lasers over against singlemode lasers.

4.2.1 *Gain guiding and index guiding lasers.* — In gain guiding lasers, the current is injected over a narrow central region using a stripe contact. The lateral variation of the optical gain confines the optical mode to the stripe vicinity. By contrast in index guiding lasers the optical mode confinement occurs through lateral variation of the refractive index of the active layer. The optical mode structure no longer depends on the injection current.

Index guiding lasers exhibit a very high RIN at threshold, but RIN decreases more abruptly in index guiding than in gain guiding devices, in terms of a relative current normalized to the threshold current (Fig. 3). For the best index guiding lasers, RIN values lie between 1×10^{-16} and 8×10^{-16} (1/Hz) at twice the threshold. In gain guiding lasers, gain saturation and intensity stability are more difficult to obtain.

Equation (7) can give a rough justification of those experimental results at least for injection currents higher than 1.2 times the threshold current. The spontaneous emission parameter β can be up to 25 times greater in gain guiding lasers compared to index guiding lasers [7].

4.2.2 *Multimode and single mode lasers.* — In conventional lasers when the Fabry-Perot (FP) cavity is formed by cleaved facets at each end of the device, the multimode emission is a

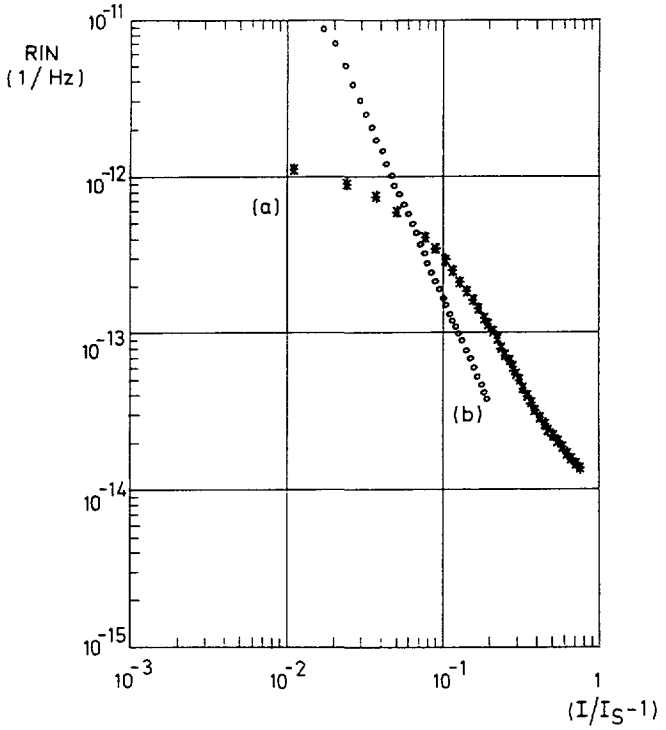

Fig. 3. — RIN at 30 MHz *versus* injection current for a gain guided laser (a) : (*) and an index guided laser (b) : (O).

consequence of the relatively broad spectrum of stimulated emission as compared to the mode spacing. In some applications like long distance optical communication systems using dispersive fibres, there is a need for a single longitudinal mode operation of laser diodes. A grating incorporated along the length of the gain region, replaces the mirrors of the Fabry-Perot cavity and provides a wavelength selective filter leading to single mode operation. But the complex building of distributed (DFB) lasers obliges many users to work with FP lasers.

In well-behaved DFB single mode lasers, RIN is smooth and decreases like $(I/I_S - 1)^{-3}$ when $I/I_S - 1$ is between 10^{-2} and 1, as predicted by relation (7). With our experimental set-up we can measure RIN values for DFB lasers, as low as 10^{-17} (1/Hz) (that is to say − 170 dB/Hz) (Fig. 5).

But a RIN increase of sometimes more than one decade occurs when a DFB laser gets two modes (Fig. 4) or when the envelope spectrum of a Fabry-Perot laser exhibits a dip. In both cases a competition between two modes settles and causes an increase of total photon number fluctuations. So there is a sharp correlation between longitudinal mode distribution and noise level [8]. As shown in figure 5, RIN values less than − 155 dB/Hz are easily obtained with an index guiding DFB laser.

Noise measurements have been carried out on a set of 26 InGaAsP index guiding lasers (Fabry-Perot and DFB types), having approximately the same active volume and emitting at 1.3 μm, carefully avoiding feedback reflections. Their structure are BH (buried heterostructure), BR (buried ridge), BC (buried crescent) and DCPBH (double channel planar BH). Their RIN measured at 20 % above threshold, that is to say for a current value where no mode competition occurs, are gathered in table I. There is no obvious correlation between RIN value and laser structure.

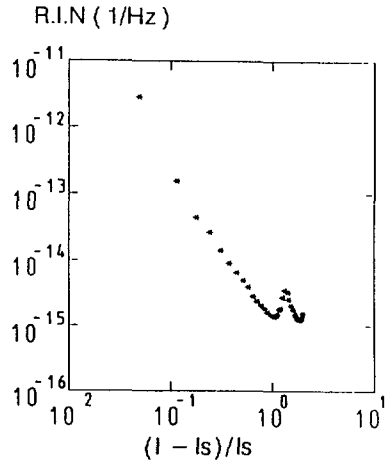

Fig. 4. — RIN plots of DFB with two modes *versus* injection current ($I/I_s - 1$).

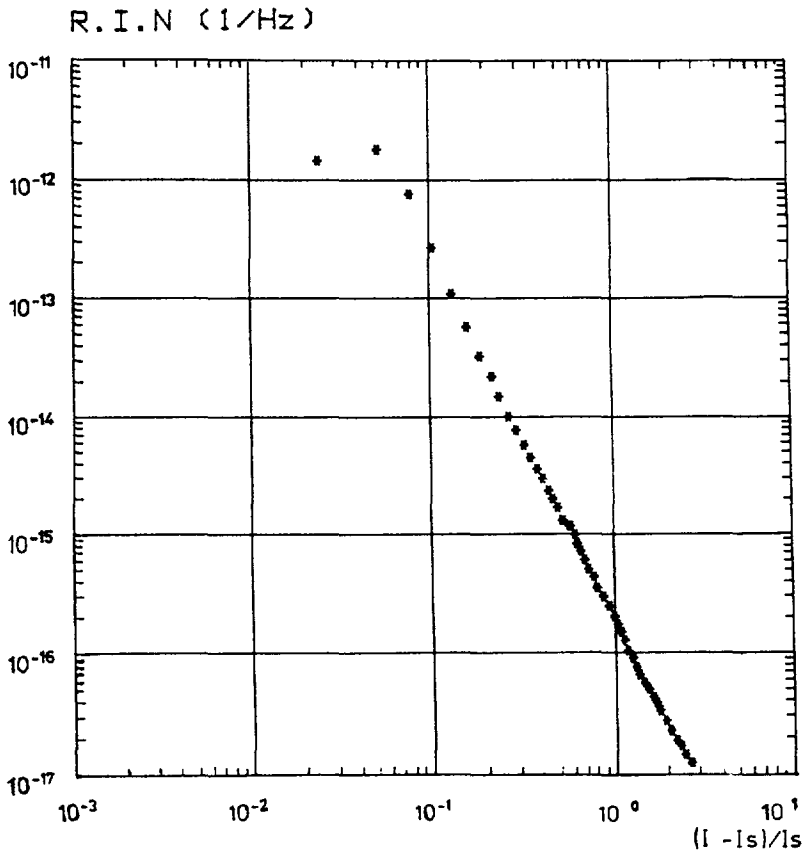

Fig. 5. — RIN of a low noise index guiding DFB laser, *versus* injection current, at 30 MHz.

Table I. — *Measured values of threshold current,* RIN *and resonance frequency at* 1.2 *the threshold current for different laser structures : 1 for grooved mesa, 2 for buried ridge, 3 for buried crescent, 4 for buried heterostructure* PPIBH, *5 for* DCPBH, *6 for double channel buried mesa. Cavity types are Perot-Fabry* (PF) *and* DFB.

Laser name	Structure n°	Cavity type	I_s (mA)	RIN 20 % 10^{-14} (Hz^{-1})	F_R 20 % (GHz)
Philips n° 77	5	PF	25	3	2.3
Philips n° 79	5	PF	23	0.5	2.2
ThCSF 302A5D	2	PF	10	4	1.6
ThCSF 304B6B	2	PF	12	0.8	2.1
ThCSF 304H7G	2	PF	11	3	1.8
ThCSF 302H3D	2	PF	12	4	1.8
LdM 1383/96M	1	PF	21	1	2
Hitachi HL1341FG	1	DFB	32	3	3.5
ATT 172	7	PF	14	3	2.1
CIT 82	1	PF	34	0.6	2.3
Fujitsu 370	5	DFB	12	2	1.7
Fujitsu 371	5	DFB	12	2	2
NEC 5600/17	6	DFB	19	3	2.4
NEC 5600/21	6	DFB	32	3	2.6
ThCSF R1BD9/09	2	PF	18	2.5	2.1
ThCSF R10A1/11	2	PF	13	2.5	3
ThCSF R181/20	2	PF	24	3	1.9
NEC 6F3911	6	PF	22	6	1.9
NEC 6F4160	6	PF	27	3	2.5
Fujitsu A10	5	DFB	16	3	1.5
Fujitsu M5	5	DFB	7	1	1.9
Fujitsu M17	5	DFB	8	2.5	1.9
Mitsubishi 7902/187	4	DFB	26	0.8	1.2
Mitsubishi 7902/192	4	DFB	12	2	1.9
Mitsubishi 7901/81	3	PF	11	3	2
Mitsubishi 7901/82	3	PF	8	1	2.1

In term of cavity length, for a set of Fabry-Perot lasers built from the same wafer, we have observed that RIN values decrease as the length of the lasers increases, as shown in figure 6. An averaging of intensity fluctuations can be imagined in a long cavity laser. So to lower the noise we can think to build long lasers but the RIN improvement is rather slim : only 4 or 5 dB between 100 μm and 400 μm length.

4.3 AT HIGH FREQUENCY. — Using our experimental set up, we follow noise variations up to 10 GHz. In figure 7, we can notice the resonant peak, the frequency of which depends on the injected current according to the simplified relation [5].

Knowledge of the intrinsic frequency response of semiconductor lasers is of basic importance in many applications [9]. If the frequency response is measured using direct current modulation, the laser diode's intrinsic response is usually masked by electrical

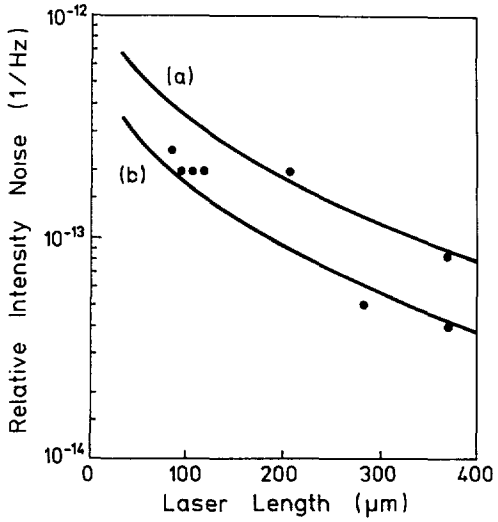

Fig. 6. — RIN *versus* laser length (L in μm) for $I = 1.1 \times I_s$. (•) : measurements at 30 MHz, (——) : theoretical curve with a spontaneous emission factor : (a) $\beta = \{0.026/L\ (\mu m)\}$. (b) $\beta = \{0.013/L\ (\mu m)\}$.

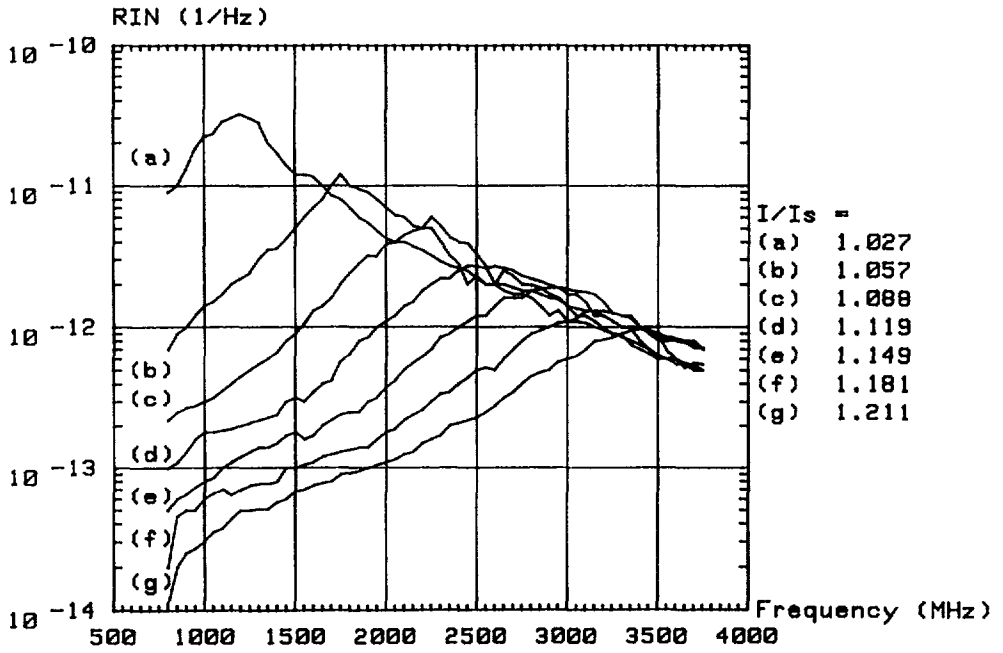

Fig. 7. — RIN *versus* frequency for different values of injection current.

parasitic elements including active layer space charge capacity, substrate elements, bond wire elements, and stub parasitic capacitance [10]. According to rate equation analysis, resonance frequency and damping factor are the same in intrinsic frequency response and in intensity noise. Since the noise is internally generated and is not filtered through the parasitic elements, noise measurements give the true intrinsic peak frequency and the true damping factor.

There is a simple relation between the damping factor Θ (related to the width of the resonance peak) and the squared resonance frequency [6]. This ratio only depends on material parameters and is two or three times higher in conventional double heterostructure lasers (DH) than in multiple quantum wells lasers (MQW), according to our measurements : 0.2 ns for DH lasers and 0.6 ns for MQW lasers. This high nonlinear damping due to spectral hole burning can limit the maximum bandwidth of MQW lasers. Resonance frequency and damping factor are plotted in figure 8. Discrepancy from relation [5] law is explained by non linear gain and gain compression.

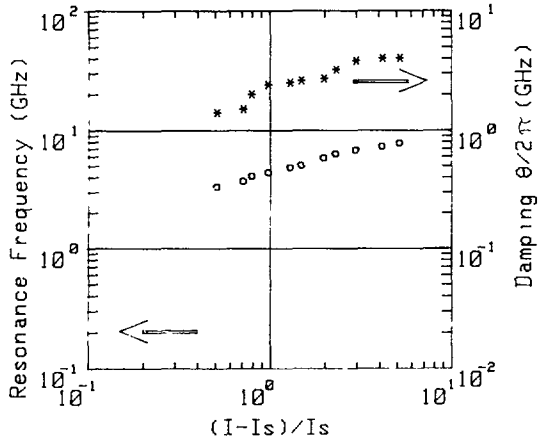

Fig. 8. — Resonance frequency (O) and damping (*) *versus* injection current.

5. Partition noise and cross-correlation coefficients between mode fluctuations.

In multimode lasers, the energy emitted by the laser is shared between the different modes. The total radiated power fluctuations are 1 000 times smaller compared to the fluctuations of an isolated mode power. This extra noise induced by the share of intensity is called laser mode partition noise. RIN of the i-th mode is defined by :

$$\mathrm{RIN}_i = 2 \cdot \frac{\langle [\Delta s_i]^2 \rangle}{S_i^2} \tag{9}$$

and calculated using rate equations.

The main mode has a smaller RIN than any one of its neighbours. Among its closest neighbours, the two having the highest amplitude show also the highest RIN.

From cross-correlation coefficients of the fluctuations between two modes, we can understand the way in which the energy is shared between the modes. Cross-correlation coefficients are defined by :

$$c_{ij} = \frac{\langle \Delta s_i(\Omega) \,.\, \Delta s_j(\Omega) \rangle}{\left(\langle [\Delta s_i(\Omega)]^2 \rangle \,.\, \langle [\Delta s_j(\Omega)]^2 \rangle \right)^{\frac{1}{2}}} \tag{10}$$

and derived from rate equations.

As shown in figure 9, the cross-correlation coefficient between the main central mode numbered « 0 » and one of the subsidiary modes numbered « 1 », « 2 », « 3 »... is negative. This means that all these subsidiary modes lose or get energy from the main central mode. Subsidiary mode cross-correlation coefficients are small and positive. This means that all these subsidiary modes exhibit in-phase intensity fluctuations between each other, exchanging energy with the lasing mode essentially.

Experimentally, the longitudinal modes are separated by a spectrometer [11]. The spectrometer output slit is opened up to let two modes go through. Then the slit width is reduced to let only one of the two modes through. Cross-correlation coefficients measurements, at 30 MHz, are shown in figure 9 : (×) for (0-1) mode pair and (+) for (1-2) mode pair.

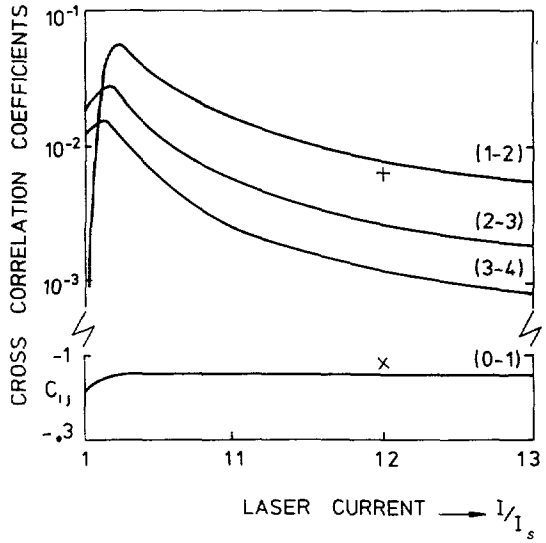

Fig. 9. — Cross-correlation coefficients as function of the injection current for four mode pairs. Solid lines : theoretical curves, (×) measurement for (0-1) mode pair. (+) measurement for (1-2) mode pair.

Conclusion.

We have presented here noise measurement results on semiconductor lasers at middle and high frequency and how they depend on the laser structure, the material properties and irregular behaviour.

From our measurements we have shown that, in analog amplitude modulation systems, it is necessary to use a DFB single mode laser to reach a RIN value less than – 155 dB/Hz and to avoid feedback reflexions.

Intensity noise measurements can still give quite a lot of informations. For instance, if we explore high frequency up to 20 GHz, we will see the ultimate intrinsic bandwidth without electrical parasitic elements. Intensity noise of isolated mode shows the way in which the total energy is shared between the different modes.

Acknowledgments.

We wish to thank C. Boisrobert for fruitful discussions and M. Dontenwille for technical assistance.

References

[1] DARCIE T. E., BODEEP G. E., Lightwave multichannel analog AM video distribution systems, ICC 89 papier 32.4.1, p. 1004, p. 1007.

[2] JOINDOT I., Bruit d'intensité relatif des lasers à semiconducteur, *Ann. Télécommun.* **46** (1991) 191-204.

[3] BORN W., WOLF G., Principes of optics (2e édition Pergamon Press, 1964).

[4] JOINDOT I., BOISROBERT C., Peculiar features of InGaAsP DH superluminescent diodes, *IEEE J. Quantum Electron.* **QE 25** (July 1989).

[5] BROSSON P., FERNIER B., LECLERC D., BENOÎT J., Carrier diffusion effects on quantum noise spectra in long wavelength BH lasers, *IEEE J. Quantum Electron.* **QE 21** (1985) 700-706.

[6] OLSHANSKY R., HILL P., LANZISERA V., POWAZINIK W., Universal relationship between resonant frequency and damping rate of 1.3 μm InGaAsP semiconductor lasers, *Appl. Phys. Lett.* **50** (March 1987).

[7] PETERMANN K., Calculated spontaneous emission factor for double heterostructure injection lasers with gain induced waveguiding, *IEEE J. Quantum Electron.* **QE 15** (1979) 566-570.

[8] JOINDOT I., BOISROBERT C., Optical spectrum irregularities and their influence on semiconductor laser intensity noise, EFOC.LAN.85 (4-4, June 19-21, 1985) Montreux Switzerland, pp. 77-80.

[9] PETERMANN K., Laser diode modulation and noise Advances in Optoelectronics (Kluwer Academic Publishers, KTK Scientific Publishers, Tokyo, 1988).

[10 ANDREKSON P., ANDERSON P., ALPING A., ENG T., *In situ* characterization of laser diodes from wide band electrical noise measurements, *IEEE J. Lightwave Technol.* **LT-4** (July 1986).

[11] JOINDOT I., BOISROBERT C., Analysis of cross-correlation between mode fluctuations in semiconductor lasers, *IEEE J. Quantum Electron.* **QE 23** (1987) 1059-1063.